Cell Reports
Article

The Multifunctional Sorting Protein PACS-2 Regulates SIRT1-Mediated Deacetylation of p53 to Modulate p21-Dependent Cell-Cycle Arrest

Katelyn M. Atkins,[1,5] Laura L. Thomas,[2,5] Jonathan Barroso-González,[2,5] Laurel Thomas,[2] Sylvain Auclair,[2] Jun Yin,[2] Hyeog Kang,[3] Jay H. Chung,[3] Jimmy D. Dikeakos,[4] and Gary Thomas[2,*]
[1]Department of Cell and Developmental Biology, Oregon Health & Science University, Portland, OR 97239, USA
[2]Department of Microbiology and Molecular Genetics, University of Pittsburgh School of Medicine, Pittsburgh, PA 15219, USA
[3]Laboratory of Obesity and Aging Research, Genetics and Development Biology Center, National Heart Lung and Blood Institute, NIH, Bethesda, MD 20892, USA
[4]Schulich School of Medicine and Dentistry, University of Western Ontario, London ON N6A 5C1, Canada
[5]Co-first author
*Correspondence: thomasg@pitt.edu
http://dx.doi.org/10.1016/j.celrep.2014.07.049

SUMMARY

SIRT1 regulates the DNA damage response by deacetylating p53, thereby repressing p53 transcriptional output. Here, we demonstrate that the sorting protein PACS-2 regulates SIRT1-mediated deacetylation of p53 to modulate the DNA damage response. PACS-2 knockdown cells failed to efficiently undergo p53-induced cell-cycle arrest in response to DNA damage. Accordingly, p53 acetylation was reduced both in PACS-2 knockdown cells and thymocytes from Pacs-2$^{-/-}$ mice, thereby blunting induction of the cyclin-dependent kinase inhibitor p21 (CDKN1A). The SIRT1 inhibitor EX-527 or SIRT1 knockdown restored p53 acetylation and p21 induction as well as p21-dependent cell-cycle arrest in PACS-2 knockdown cells. Trafficking studies revealed that cytoplasmic PACS-2 shuttled to the nucleus, where it interacted with SIRT1 and repressed SIRT1-mediated p53 deacetylation. Correspondingly, in vitro assays demonstrated that PACS-2 directly inhibited SIRT1-catalyzed p53 deacetylation. Together, these findings identify PACS-2 as an in vivo mediator of the SIRT1-p53-p21 axis that modulates the DNA damage response.

INTRODUCTION

The tumor suppressor p53 is perhaps the most frequent target of genetic lesions in human cancer. Following DNA damage, p53 orchestrates biological fates ranging from growth arrest to cell death, and the molecular pathways leading to these various outcomes depend on several factors, including the level and type of stress as well as the cell and tissue type (Mirzayans et al., 2012; Zilfou and Lowe, 2009). p53 functions as a sequence-specific transcription factor that drives the transactivation of target genes mediating cell-cycle arrest, senescence, or apoptosis induced by the intrinsic pathway (Kruse and Gu, 2009). Among the p53 target genes, perhaps the best characterized is the cyclin-dependent kinase inhibitor p21, which promotes cell-cycle arrest, supports DNA damage repair, and impedes apoptosis (Abbas and Dutta, 2009). In addition, p53 integrates the intrinsic apoptotic pathway with the extrinsic apoptotic pathway triggered by the death ligand TRAIL. Indeed, tumor cell apoptosis can be increased when TRAIL is combined with DNA damage-inducing therapies (Ifeadi and Garnett-Benson, 2012).

The transcriptional activity of p53 is critically dependent on posttranslational modifications, including phosphorylation and acetylation, which stabilize p53 and enhance its transactivation functions, respectively (Kruse and Gu, 2009). Acetylation of p53 is catalyzed predominantly by the histone acetyltransferase p300 (Gu and Roeder, 1997). Indeed, stress-induced p53 acetylation significantly correlates with p53 activation (Kruse and Gu, 2009; Zilfou and Lowe, 2009). Accordingly, mutation of all major lysine acetylation sites blocks the ability of p53 to induce p21 and suppress cell proliferation, suggesting that acetylation of p53 is indispensable for the p53-p21 pathway (Tang et al., 2008). Conversely, the class III histone deacetylase (HDAC) SIRT1 inhibits p53 transcriptional activation by deacetylating p53 following DNA damage (Kruse and Gu, 2009). Together, the overall balance of p300 and SIRT1 activities modulates p53 transcriptional function.

Although regulation of p53 by modifying enzymes and cofactors has been extensively studied, less is known about the regulation of SIRT1. Gene expression of SIRT1 can be regulated transcriptionally and posttranscriptionally (Kwon and Ott, 2008). In addition, SIRT1 deacetylase activity can be modulated by interaction with cellular proteins (Hasegawa and Yoshikawa, 2008; Kim et al., 2007, 2008; Liu et al., 2011; Zhao et al., 2008). Although these studies provide insight into

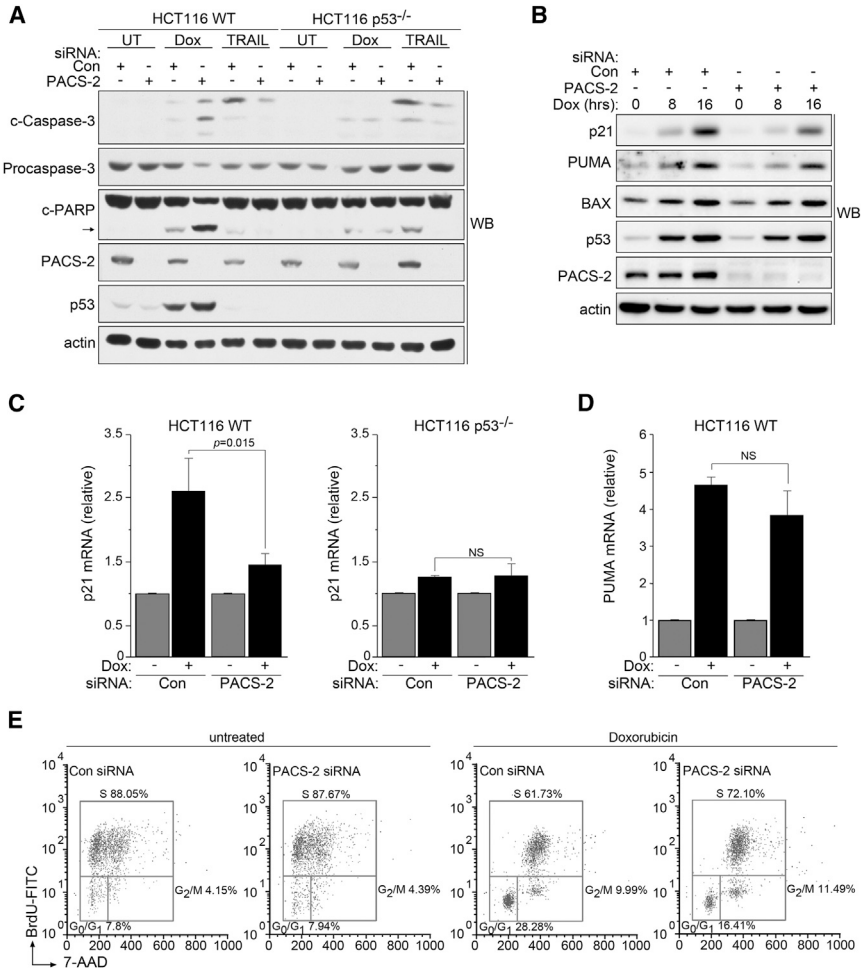

Figure 1. PACS-2-Deficient Cells Have Reduced p21-Dependent Cell-Cycle Arrest following DNA Damage

(A) Control (Con) or PACS-2 siRNA-treated HCT116 WT or p53$^{-/-}$ cells were treated with 0.5 μM Dox for 48 hr or 20 ng/ml TRAIL for 5 hr prior to harvest and analyzed by western blot (WB). The cleaved caspase-3 antibody detected 19, 17, and 15 kDa forms. Arrow denotes cleaved poly(ADP ribose) polymerase (PARP). UT, untreated.

(B) Control (Con) or PACS-2 siRNA-treated HCT116 cells were treated with 0.5 μM Dox and analyzed by western blot. Quantification using AlphaView (ProteinSimple) showed that after 16 hr Dox treatment, PACS-2 knockdown reduced p21 by 50%, whereas PUMA and Bax were less affected (16% and 12% reduction, respectively).

(C) Control (Con) or PACS-2 siRNA-treated HCT116 WT (left) or HCT116 p53$^{-/-}$ (right) cells were treated with 0.5 μM Dox (4 hr) and analyzed by qPCR (normalized to glyceraldehyde 3-phosphate dehydrogenase [GAPDH]). Error bars represent mean ± SD from three or more independent experiments. Statistical significance was determined using Student's t test. NS, not significant.

(D) HCT116 WT cells from (B) were analyzed for PUMA mRNA by qPCR (normalized to GAPDH). Error bars represent mean ± SD from four independent experiments. Statistical significance was determined using Student's t test.

(E) Synchronized control (Con) or PACS-2 siRNA-treated HCT116 cells were stimulated to reenter the cell cycle in the presence of 10 μM BrdU, treated with 0.5 μM Dox (24 hr), and processed for flow cytometry. Results are representative of three independent experiments.

See also Table S1 and Figures S1 and S2.

the regulation of SIRT1, the diversity of SIRT1 substrates in pathways ranging from DNA damage and cell survival to glucose and lipid homeostasis suggests that regulation of SIRT1 activity is complex and likely requires additional cellular factors (Brooks and Gu, 2009).

Here, we identify the multifunctional sorting protein PACS-2 as an inhibitor of SIRT1-mediated deacetylation of p53 following DNA damage. PACS-2 was initially identified by its role in mediating secretory pathway traffic and formation of contacts between the endoplasmic reticulum and mitochondria (*m*itochondria-*a*ssociated *m*embranes or MAMs) to regulate interorganellar communication and autophagy (Atkins et al., 2008; Dikeakos et al., 2012; Hamasaki et al., 2013; Köttgen et al., 2005; Simmen et al., 2005). In response to TRAIL, however, PACS-2 switches to a proapoptotic effector that coordinates trafficking steps leading to mitochondria membrane permeabilization and activation of executioner caspases (Aslan et al., 2009; Werneburg et al., 2012). In this study, we show that, contrary to its role in TRAIL action, PACS-2 responds to DNA damage by regulating the extent of SIRT1-mediated deacetylation of p53 to induce p21-dependent cell-cycle arrest. Together, these findings suggest that PACS-2 is a regulator of the SIRT1-p53-p21 axis that modulates the DNA damage response.

RESULTS

PACS-2 Mediates the p53-Dependent Response to DNA Damage

Previous studies identified an essential role for cytoplasmic PACS-2 in mediating TRAIL-induced apoptosis (Aslan et al., 2009; Werneburg et al., 2012). To determine whether this proapoptotic requirement for PACS-2 extended to DNA damage, we compared the effect of PACS-2 knockdown on TRAIL- versus doxorubicin (Dox)-induced apoptosis in HCT116 wild-type (WT) or isogenic p53$^{-/-}$ cells (Figure 1A). As expected, PACS-2 knockdown blunted TRAIL-induced apoptosis independent of p53 status. By contrast, PACS-2 knockdown sensitized HCT116 WT cells but not p53$^{-/-}$ cells to Dox-induced apoptosis (Figures 1A and S1A). This effect additionally required the proapoptotic p53 target PUMA and was also observed using ionizing radiation (IR; Figures S1B and S1C). These findings suggest

distinct roles for PACS-2 in TRAIL- versus p53-mediated apoptosis.

PACS-2 Regulates p53-Mediated Cell-Cycle Arrest following DNA Damage

The increased sensitivity of PACS-2-deficient cells to p53- and PUMA-mediated apoptosis following DNA damage led us to ask whether PACS-2 knockdown altered induction of p53 target genes. Analysis by western blot showed that PACS-2 knockdown reduced the p53-dependent induction of p21 but had little effect on the proapoptotic targets PUMA or Bax (Figure 1B). These findings were consistent with quantitative PCR (qPCR) analysis, which showed that PACS-2 knockdown reduced the p53-dependent induction of p21 by approximately 40% (Figure 1C). MDM2 and Noxa were reduced to a lesser extent, 27% and 19%, respectively, whereas there was no significant reduction in PUMA, Bax, DR5, 14-3-3, or Gadd45a (Figures 1D and S2A). Similar results were observed in U2OS cells following IR, demonstrating that this effect of PACS-2 knockdown on p21 induction was not restricted to a single cell line or treatment (Figure S2B).

The blunted induction of p21 following DNA damage in PACS-2 knockdown cells led us to test the role of PACS-2 in mediating DNA damage-induced cell-cycle arrest. As expected, PACS-2 knockdown significantly reduced the percentage of HCT116 WT cells in G_0/G_1 compared to control cells following treatment with Dox (Figure 1E; Table S1). Because p21 has well-described roles in promoting growth arrest and repressing apoptosis following DNA damage (Mirzayans et al., 2012), we tested whether the repressed induction of p21 in PACS-2 knockdown HCT116 WT cells contributed to their increased sensitivity to DNA damage. Similar to PACS-2 knockdown, p21 knockdown sensitized HCT116 cells to Dox-induced apoptosis (Figure S2C). Consistent with this finding, knockdown of PACS-2 in isogenic HCT116 $p21^{-/-}$ cells failed to further sensitize them to Dox-induced apoptosis compared to control cells (Figure S2D). Together, these findings suggest that the disparate p53-dependent induction of p21 versus PUMA in PACS-2-depleted cells resulted in reduced G_1 arrest and a corresponding increase in apoptosis. These findings further suggest that PACS-2 and p21 may participate in a common pathway to promote cell-cycle arrest.

PACS-2 Regulates the p53-p21 Axis In Vivo following DNA Damage

Consistent with the results from both HCT116 and U2OS cells, Pacs-$2^{-/-}$ thymocytes contained reduced levels of p21 protein and mRNA following exposure to IR (Figures 2A and 2B, and see Figure 1). The predisposition of thymocytes to undergo apoptosis in response to IR precluded evaluation of cell-cycle arrest. By contrast, p53-mediated p21 induction plays an essential role in mitigating GI toxicity following IR by inducing cell-cycle arrest to restrict enterocyte migration along the crypt-villus axis (Komarova et al., 2004; Leibowitz et al., 2011; Li et al., 2005; Sullivan et al., 2012). Consistent with these studies, we found that migration of bromodeoxyuridine-positive ($BrdU^+$) enterocytes was restricted in WT mice but not Pacs-$2^{-/-}$ mice following IR (Figure 2C).

PACS-2 Modulates p53 Acetylation In Vivo following DNA Damage

The determination that PACS-2 knockdown repressed p21 induction but had no significant effect on total p53 levels (see Figures 1B, 2A, and 2D) suggested that PACS-2 might modulate p53 activation by controlling p53 posttranslational modifications. Therefore, we analyzed the extent of p53 Lys_{382} acetylation, which correlates with p53 activation and p21 induction (Wang et al., 2008), and p53 Ser_{15} phosphorylation, which promotes p53 stabilization and interaction with p300 (Lee et al., 2010), in control or PACS-2 knockdown HCT116 cells following Dox treatment. Strikingly, PACS-2 knockdown reduced endogenous p53 Lys_{382} acetylation, but not Ser_{15} phosphorylation (Figure 2D). Similar results were obtained in Pacs-$2^{-/-}$ thymocytes where acetylation of p53 Lys_{379} (equivalent to human p53 Lys_{382}) was reduced 60%, whereas p53 $pSer_{18}$ (equivalent to human p53 Ser_{15}) was unaffected (Figure 2A). Additionally, p53 acetylation and p21 induction were blunted in PACS-2 knockdown cells following treatment with the MDM2 antagonist, Nutlin-3a, which triggers p53-dependent induction of p21 independent of DNA damage (Figure S3; Kumamoto et al., 2008). Together, these results suggest that PACS-2 mediates induction of a subset of p53 target genes by controlling p53 acetylation.

PACS-2 Controls the Extent of Acetylated p53 Bound to the p21 Promoter following DNA Damage

p53 acetylation is a crucial regulatory element controlling transactivation of p53 target genes. Therefore, we performed chromatin immunoprecipitation (ChIP) to analyze the amount of total and acetylated p53 bound to the p21 promoter following DNA damage (Figure 2E). Indeed, PACS-2 knockdown reduced the extent of acetylated p53, but not total p53, bound to the p21 promoter following DNA damage. These findings suggest that PACS-2 loss does not impede binding of p53 to target DNA sequences but, instead, diminishes the extent to which promoter-bound p53 is acetylated and, therefore, transcriptionally active.

PACS-2 Traffics to the Nucleus and Interacts with SIRT1

The determination that loss of PACS-2 reduced the level of acetylated p53 bound to the p21 promoter led us to ask whether PACS-2 modulates p53 acetylation by interacting with p300 or SIRT1. Coimmunoprecipitation analyses demonstrated that PACS-2 interacted with SIRT1 and that the endogenous SIRT1-PACS-2 interaction was increased following Dox treatment (Figures 3A and 3B).

Whereas SIRT1 deacetylates histones and transcription factors in the nucleus, PACS function has thus far been studied solely in the regulation of membrane traffic in the cytoplasm (Brooks and Gu, 2009; Youker et al., 2009). Inspection of the PACS-2 sequence, however, revealed multiple candidate leucine-rich nuclear export signals (NESs; see Figure 7A; la Cour et al., 2004; Youker et al., 2009). Indeed, treatment with the nuclear export inhibitor Leptomycin B (LMB) led to nuclear accumulation of PACS-2 (Figure 3C). Whereas PACS-2 lacks a predicted nuclear localization signal (NLS), the PACS-2 paralog, PACS-1, contains a canonical NLS (..$VKKTRRKL_{318}$..) and readily distributes between the cytoplasm and nucleus (Figure 3C; see Discussion). The homologous sequence in PACS-2

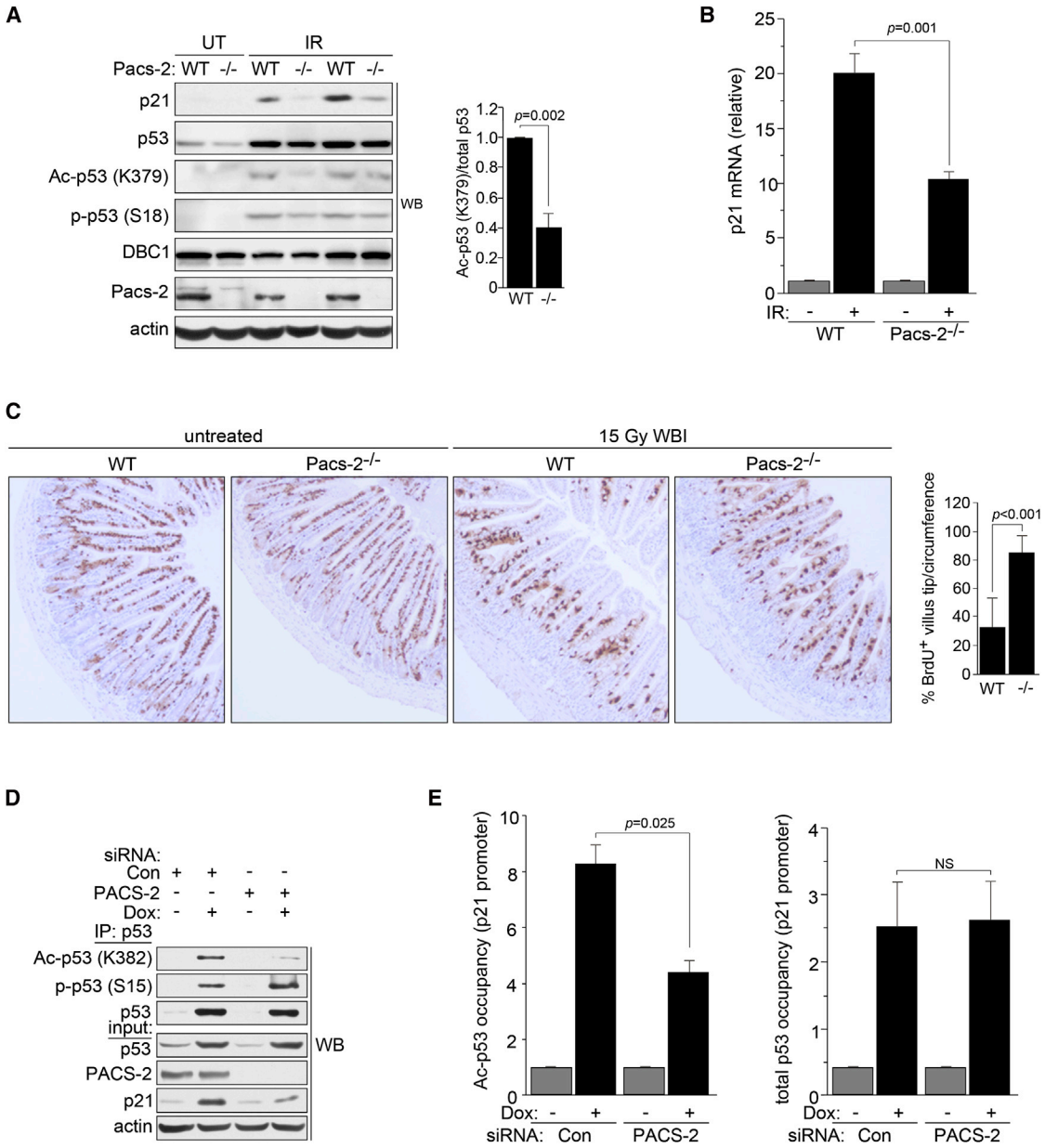

Figure 2. PACS-2 Modulates p53 Acetylation In Vivo following DNA Damage

(A) Left: thymuses from WT and Pacs-2$^{-/-}$ (−/−) mice exposed or not to 4.5 Gy IR (6 hr) were analyzed by western blot. In the right panel, Ac-p53 (K_{379}) and total p53 were quantified using NIH ImageJ from IR-exposed WT or Pacs-2$^{-/-}$ mice. Error bars represent mean ± SEM from four mice per condition. Statistical significance was determined using Student's t test.

(B) Thymuses from WT and Pacs-2$^{-/-}$ mice exposed to 4.5 Gy IR (6 hr) as indicated were analyzed for p21 induction by qPCR (normalized to GAPDH). Error bars represent mean ± SEM from four or more mice per condition. Statistical significance was determined using Student's t test.

(C) Left: small intestines from WT and Pacs-2$^{-/-}$ (−/−) mice were analyzed by IHC for BrdU 48 hr following labeling and exposure to 15 Gy WBI as indicated. In the right panel, the percentage of BrdU^{+} cells reaching the upper one-fourth of the villus tips per circumference was quantified. Error bars represent mean ± SD. Statistical significance was determined using Student's t test. Quantification from untreated mice was not determined because all villus tips from these mice contained BrdU^{+} cells.

(D) p53 was immunoprecipitated from Control (Con) or PACS-2 siRNA-treated HCT116 cells treated with 0.5 μM Dox and analyzed by western blot.

(E) Control (Con) or PACS-2 siRNA-treated HCT116 cells treated with 0.5 μM Dox (6 hr) were analyzed by ChIP qPCR for the p21 promoter using antibodies specific for total p53 (DO-1) or Ac-p53 (K_{382}). Error bars represent mean ± SEM from three independent experiments. Statistical significance was determined using Student's t test. NS, not significant.

See also Figure S3.

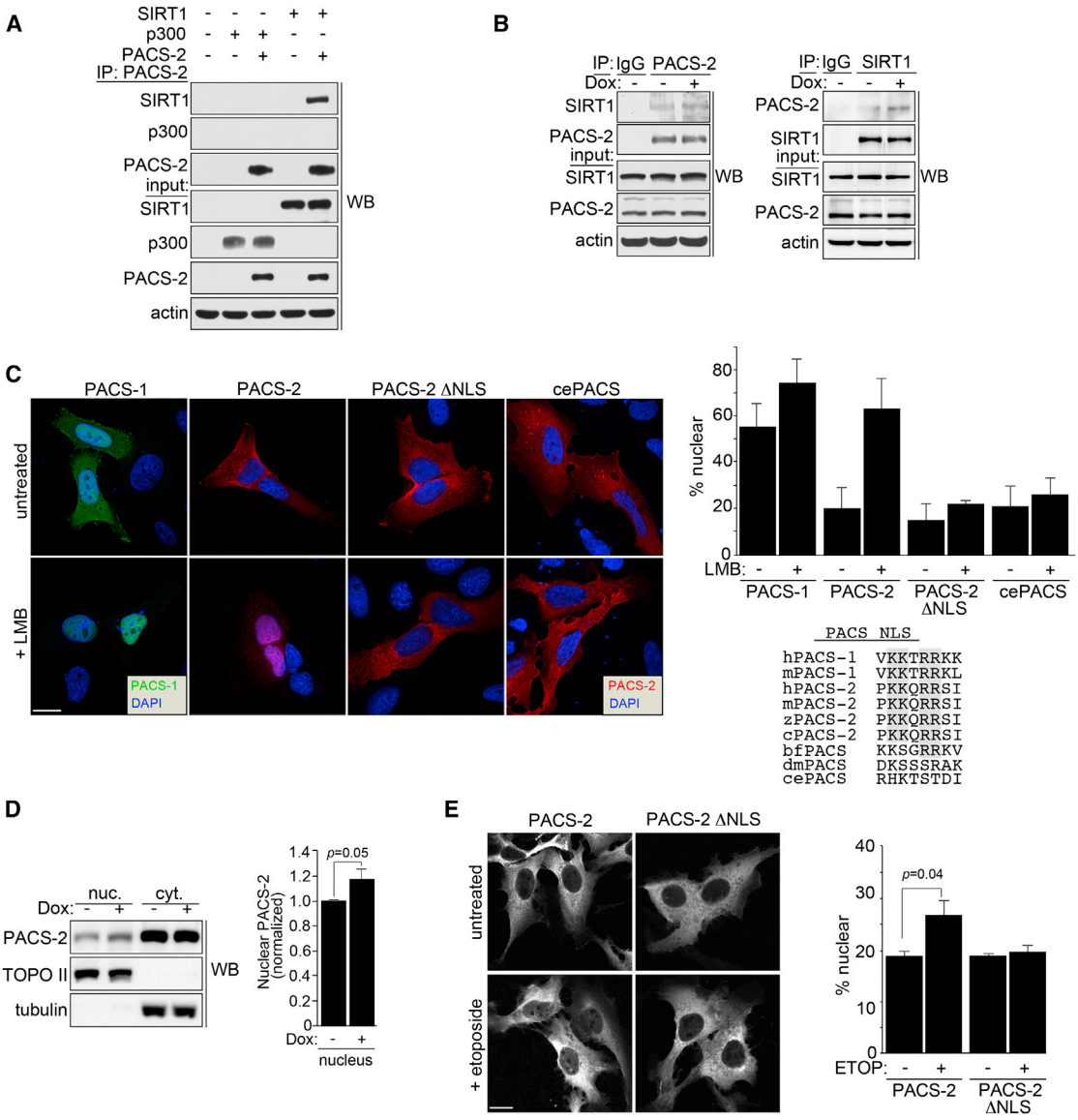

Figure 3. PACS-2 Interacts with SIRT1 in the Nucleus

(A) PACS-2-FLAG was immunoprecipitated (IP) from HCT116 cells, and coprecipitating SIRT1-V5 or p300-HA was detected by western blot.

(B) HCT116 cells treated with 0.5 μM Dox (3 hr) as indicated were immunoprecipitated with control immunoglobulin G, anti-PACS-2 (left), or anti-SIRT1 (right), and coprecipitating SIRT1 (left) or PACS-2 (right) was detected by western blot.

(C) Left: U2OS cells expressing EGFP-PACS-1, mCherry-PACS-2, mCherry-PACS-2ΔNLS, or mCherry *C. elegans* PACS (T18H9.7a) were treated with 40 nM LMB (3 hr) and analyzed by deconvolution microscopy. Nuclei were stained with DAPI. In the top-right panel, percent total cellular fluorescent protein signal in the nucleus was quantified. Error bars represent mean ± SD from >100 cells in 3 independent experiments. Bottom-right panel shows alignment of the predicted NLS motif (https://www.predictprotein.org) fitting the consensus *[PLV]K[RK]x[RK][RK][RK][PL]* from hPACS-1 (sp|Q6VY07, gi|30089916) with hPACS-2 (sp|Q86VP3, gi|155029546), mouse PACS-1 (gi|54291704), mouse PACS-2 (kkqrrsiv, gi|124487181), chicken PACS-2 (gi|513196172), zebrafish PACS-2 (gi|170172595), amphioxus PACS (gi|229298623), *Drosophila* PACS (Krt95D, gi|24649488) and *C. elegans* PACS (T18H9.7a, gi|373219078). Consensus basic amino acid doublets are shaded.

(D) HCT116 cells were treated or not with 0.5 μM Dox for 6 hr. PACS-2 in the nuclear (nuc.) and cytoplasmic (cyt.) fractions was detected by western blot. Error bars represent mean ± SD from three independent experiments. Statistical significance was determined using Student's t test.

(E) U2OS cells expressing mCherry-PACS-2 or mCherry-PACS-2ΔNLS were treated with 100 μM etoposide (3 hr) and analyzed by confocal microscopy. Nuclei were stained with DAPI. In the bottom panel, percent total cellular fluorescent protein signal in the nucleus was quantified. Error bars represent mean ± SD from >100 cells in 3 independent experiments. Scale bar, 10 μm.

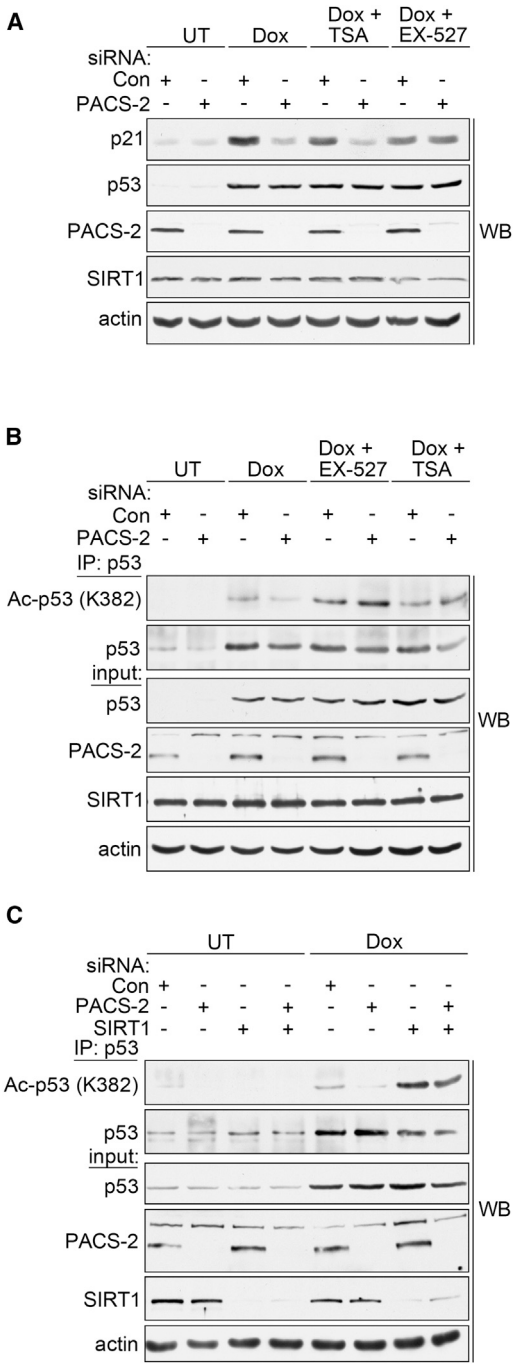

Figure 4. PACS-2 Regulates SIRT1-Mediated Deacetylation of p53 In Vivo

(A) Control (Con) or PACS-2 siRNA-treated HCT116 cells were treated with 0.5 μM Dox (6 hr) alone or with 0.5 μM TSA or 1 μM EX-527 and analyzed by western blot.

(B) Control (Con) or PACS-2 siRNA-treated HCT116 cells were treated as in (A); total p53 immunoprecipitated with anti-p53 (DO-1) and Ac-p53 (K_{382}) or total p53 (FL-393) was detected by western blot.

(C) HCT116 cells transfected with control (Con), PACS-2, or SIRT1 siRNAs were processed as in (B).

(..PKKQRRSI$_{239}$..), when mutated (RR$_{237}$→AA, hereafter called PACS-2ΔNLS), was unaffected by LMB, suggesting that this motif is required for nuclear localization of PACS-2 (Figure 3C). PACS sequence alignment suggests that nuclear-trafficking motifs appeared later in evolution because *C. elegans* PACS lacks a predicted NLS and failed to accumulate in the nucleus (Figure 3C). Treatment with Dox or etoposide increased nuclear localization of PACS-2, suggesting that a fraction of PACS-2 enters the nucleus to regulate SIRT1 following DNA damage (Figures 3D and 3E). The reduced nuclear accumulation of mCherry-PACS-2 in response to DNA damage compared to LMB may reflect differences in the signaling pathways that control nuclear accumulation in response to DNA damage compared to a pharmacologic block of CRM1-dependent nuclear export.

PACS-2 Regulates SIRT1-Mediated Deacetylation of p53 to Induce p21-Dependent Cell-Cycle Arrest

The reduced acetylation of p53 in PACS-2-deficient cells following DNA damage together with the DNA damage-induced interaction between PACS-2 and SIRT1 (Figures 1, 2, and 3) led us to ask whether PACS-2 mediates p21 induction by regulating SIRT1-dependent deacetylation of p53. Accordingly, control or PACS-2 knockdown HCT116 cells were treated with Dox in the absence or presence of the class I/class II HDAC inhibitor trichostatin A (TSA), which does not inhibit the class III HDAC SIRT1, or with the SIRT1-specific inhibitor EX-527 (Napper et al., 2005; Solomon et al., 2006). As expected (see Figures 1 and 2), PACS-2 knockdown reduced Dox-mediated induction of p21, and this effect was abrogated by EX-527, but not TSA (Figure 4A), suggesting that the reduced p21 expression in PACS-2-depleted cells was SIRT1 dependent. Moreover, in agreement with others, the reduced p53 acetylation in PACS-2-depleted cells was reversed by EX-527 or the concomitant knockdown of SIRT1 (Figures 4B and 4C; see Cheng et al., 2003; Solomon et al., 2006). The molecular basis underlying the ability of TSA to rescue p53 acetylation but not p21 induction is not known but is consistent with previous studies (Cheng et al., 2003).

The SIRT1-dependent repression of p53 acetylation and p21 expression in PACS-2 knockdown cells suggested that the subsequent reduction in p21-dependent cell-cycle arrest (see Figure 1E) might similarly be SIRT1 dependent. Indeed, treatment of PACS-2 knockdown cells with EX-527 restored p21-dependent cell-cycle arrest and p21 expression (Figures 5A–5C; Table S2). Importantly, the effect of SIRT1 inhibition was dependent on PACS-2 knockdown because both the extent of p21 induction and G_1 arrest were not significantly affected by EX-527 in control cells. Moreover, EX-527 failed to increase the extent of G_1 arrest in p21 knockdown cells, demonstrating that the cell-cycle arrest rescued by the SIRT1 inhibitor in PACS-2 knockdown cells was p21 dependent. Together, these data suggest that PACS-2 regulates the ability of SIRT1 to deacetylate p53 following DNA damage, thereby promoting p21 induction and p21-dependent cell-cycle arrest.

PACS-2 Inhibits SIRT1-Mediated Deacetylation of p53

The SIRT1-dependent reduction of acetylated p53 and thus p21 expression in PACS-2-deficient cells suggested that PACS-2 promotes p53 activation by regulating SIRT1 deacetylase

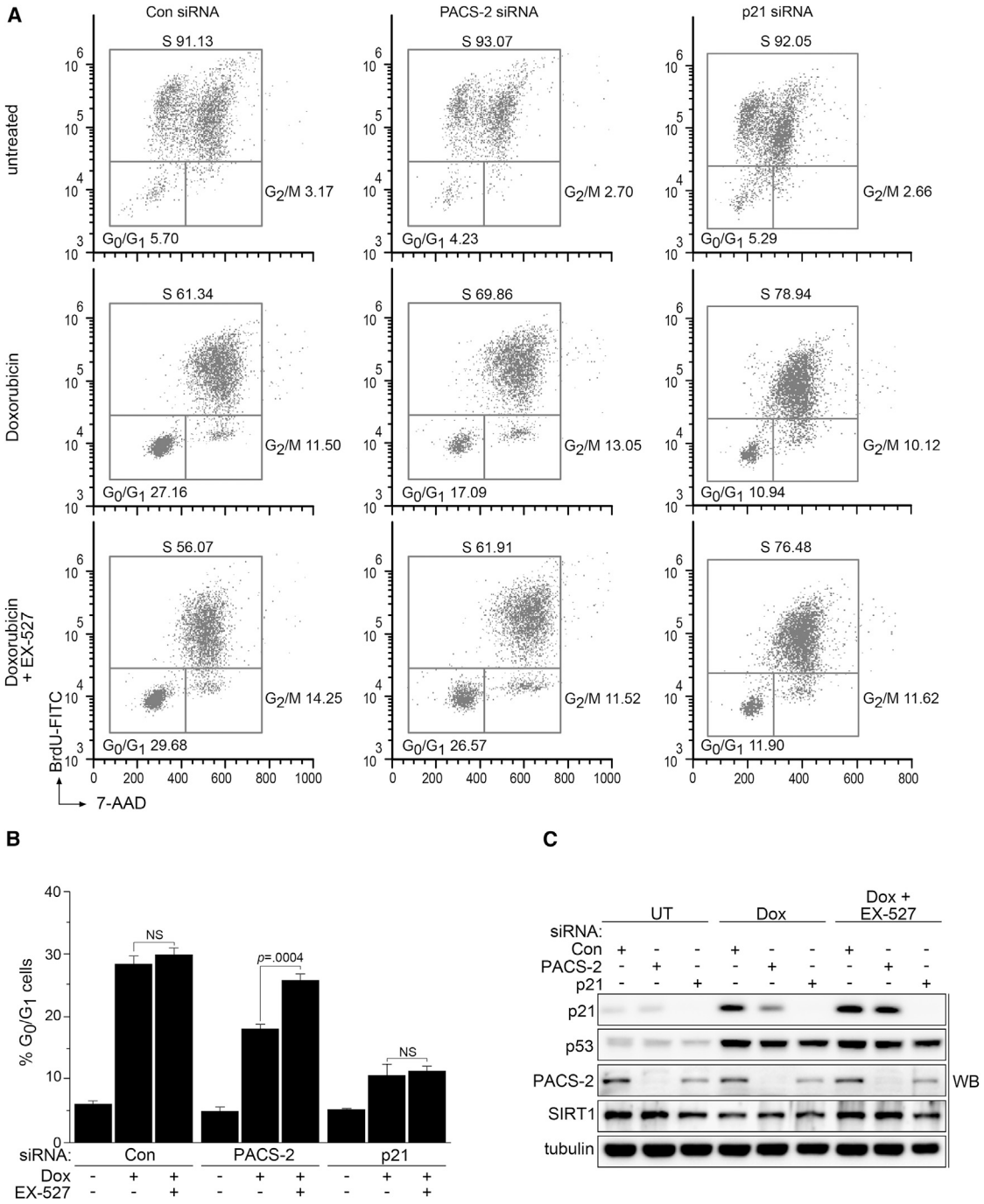

Figure 5. Inhibition of SIRT1 Restores p21-Dependent Cell-Cycle Arrest in PACS-2 Knockdown Cells

(A) Synchronized control (Con), PACS-2, or p21 siRNA-treated HCT116 cells were stimulated to reenter the cell cycle with 10% FBS in the presence of 10 μM BrdU and then treated or not with 0.5 μM Dox (24 hr) in the presence or absence of 10 μM EX-527 and processed for flow cytometry. Results are representative of three independent experiments.

(B) Quantitation of cells from (A) arrested in G_0/G_1. Error bars represent mean ± SEM from three independent experiments. Statistical significance was determined using Student's t test. NS, not significant.

(C) Lysates from (A) were analyzed for the indicated proteins by western blot.

See also Table S2.

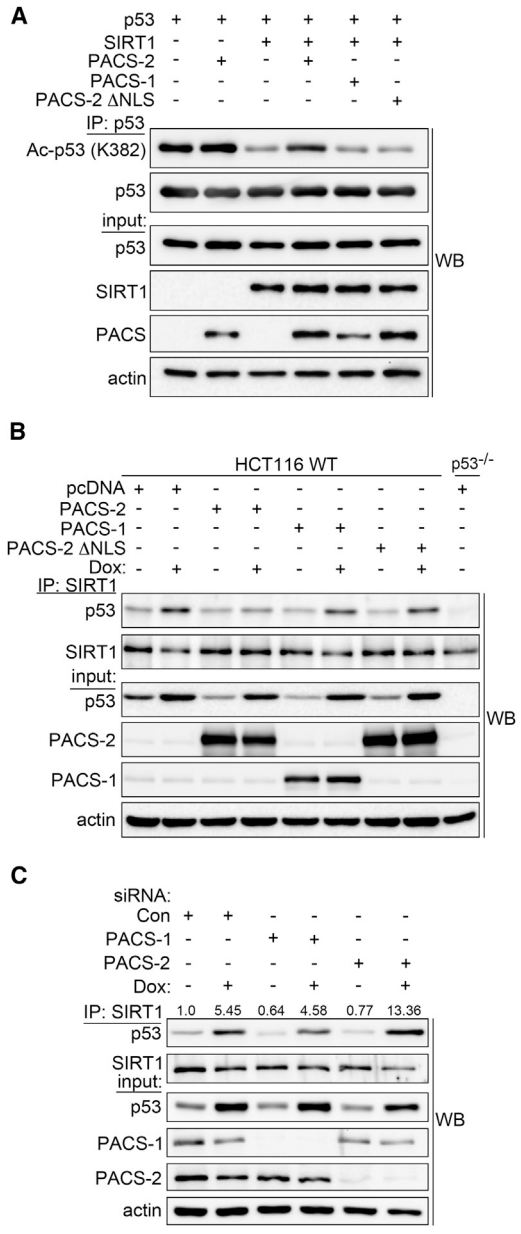

Figure 6. Nuclear PACS-2 Regulates the p53-SIRT1 Interaction

(A) Total p53 was immunoprecipitated from HCT116 cells, and Ac-p53 (K_{382}) was analyzed by western blot.

(B) Endogenous SIRT1 was immunoprecipitated from HCT116 WT or $p53^{-/-}$ cells treated with 0.5 μM Dox (6 hr) as indicated, and coprecipitating p53 was analyzed by western blot.

(C) HCT116 cells were treated with 0.5 μM Dox (14 hr), and endogenous SIRT1 immunoprecipitated and coprecipitating p53 were analyzed by western blot. p53 was quantified using AlphaView (ProteinSimple).

activity. Consistent with this possibility, PACS-2, but not PACS-2ΔNLS or PACS-1, inhibited SIRT1-dependent p53 deacetylation (Figure 6A). Interestingly, PACS-2, but not PACS-2ΔNLS or PACS-1, blocked the DNA damage-induced interaction between endogenous SIRT1 and p53 (Figure 6B), whereas knockdown of PACS-2 increased the interaction (Figure 6C). Together, these studies suggest that following DNA damage, PACS-2 localizes to the nucleus where it regulates the interaction between SIRT1 and p53 to promote p53 acetylation.

Next, we tested whether PACS-2 could bind SIRT1 and directly inhibit SIRT1-mediated deacetylation of p53 in vitro. We found that SIRT1 bound specifically to the PACS-2 cargo(furin)-binding region ($PACS\text{-}2_{FBR}$, Figure 7A). Conversely, the $PACS\text{-}2_{FBR}$ preferentially bound the SIRT1 N-terminal region (NT; Figure 7B) but interacted weakly with a catalytically active SIRT1 construct lacking the NT (SIRT1-ΔNT, Figure S4A; see Experimental Procedures). Importantly, $PACS\text{-}2_{FBR}$ inhibited the ability of full-length SIRT1, but not SIRT1-ΔNT, to deacetylate p53 in a nicotinamide adenine dinucleotide (NAD^+)- and dose-dependent manner (Figure 7C). Moreover, full-length PACS-2 bound SIRT1, but not the p53 substrate, and inhibited the ability of SIRT1 to deacetylate p53 in vitro (Figures 7D, S4B, and S4C). By contrast, full-length PACS-1, which also bound SIRT1, had no measurable effect on SIRT1 activity (see Figure 6). Together, these results suggest that PACS-2 regulates p53-mediated p21 induction following DNA damage by controlling SIRT1-mediated deacetylation of p53.

DISCUSSION

The balance between cytostasis and apoptosis is a key determinant of cell fate following DNA damage. The selective repression of p53-mediated p21 induction shifts the DNA damage response from cytostasis to PUMA-dependent apoptosis (Haupt et al., 2003; Seoane et al., 2002). Whereas the most well-characterized role of p21 is the execution of p53-dependent cell-cycle arrest, p21 also directly antagonizes PUMA- and Bax-mediated apoptosis by preventing procaspase-3 activation and by repressing procaspase-2 expression (Baptiste-Okoh et al., 2008; Hill et al., 2011; Suzuki et al., 2000; Yu et al., 2003). Thus, our determination that following DNA damage PACS-2 knockdown cells have repressed induction of p21 but not PUMA or Bax, as well as increased apoptosis, suggests that PACS-2 inhibits SIRT1 to selectively promote p21-dependent cytoprotective functions of the p53-dependent DNA damage response.

SIRT1 is frequently reported to delay aging by promoting cell survival (Brooks and Gu, 2009; Cheng et al., 2003; Cohen et al., 2004). Thus, our determination that PACS-2 knockdown leads to a SIRT1-dependent reduction in p53 acetylation and p21 expression as well as sensitization of cells to DNA damage-induced apoptosis appears inconsistent with a cytoprotective role for SIRT1. The well-established antiaging roles for SIRT1, however, may not necessarily correlate with a cytoprotective role following DNA damage. Indeed, deletion of p21 improves stem cell maintenance and increases lifespan, whereas induction of p21 protects adult stem cells from acute genotoxic stress but impairs stem cell survival in the context of age-associated chronic DNA damage (Ju et al., 2007; Mantel and Broxmeyer, 2008; Sperka et al., 2012). To what extent these findings in stem cells extend to cancer cells warrants investigation.

The role of SIRT1 in tumor cell survival and cancer progression is controversial because SIRT1 has both tumor-promoting and

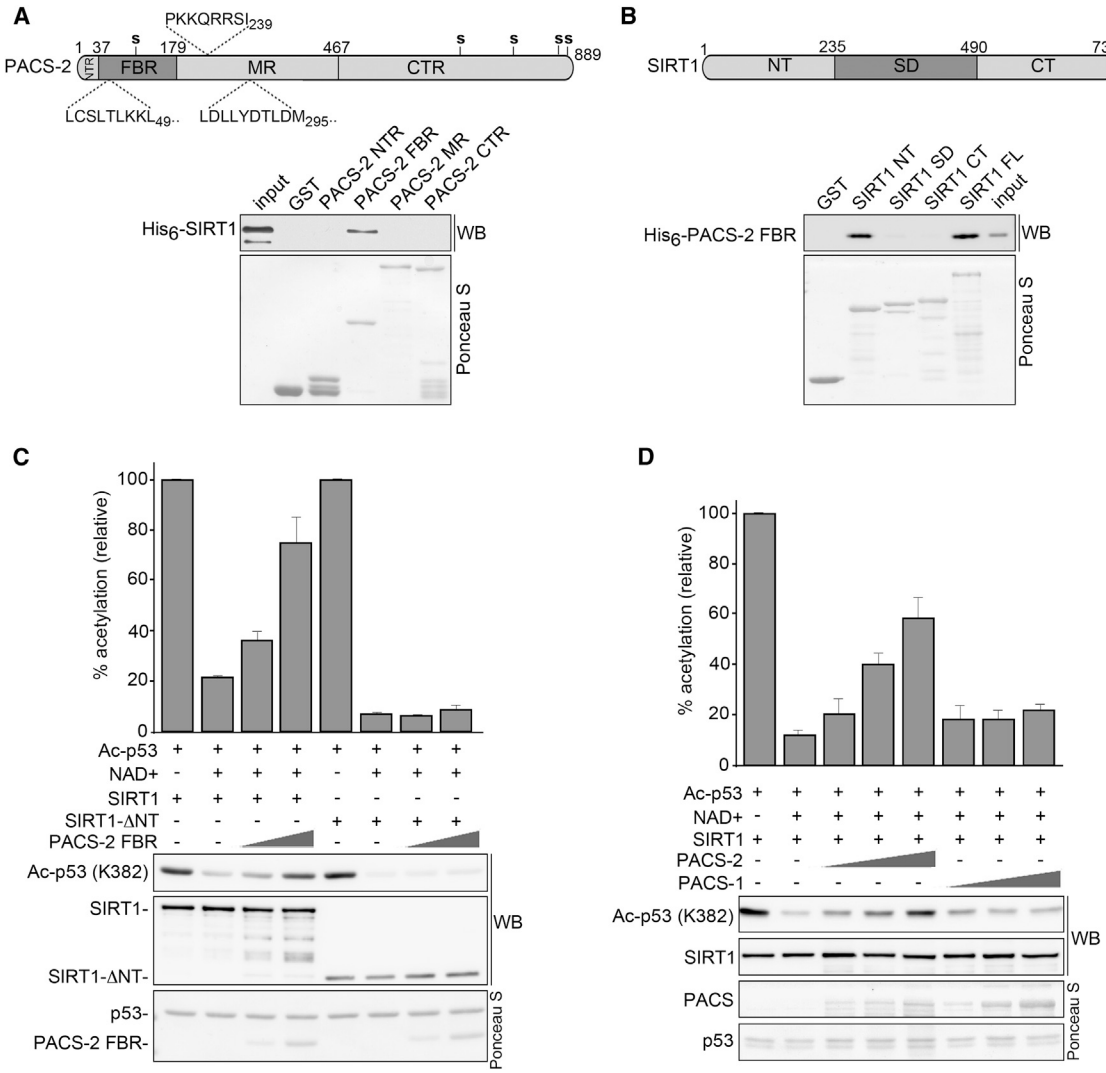

Figure 7. PACS-2 Inhibits SIRT1-Mediated Deacetylation of p53 In Vitro

(A) Top: schematic of hPACS-2 and the predicted NLS (above) and NES (below). In the bottom panel, full-length His_6-SIRT1Δ_{6-83} was incubated with GST or GST-PACS-2 constructs, and interacting His_6-SIRT1Δ_{6-83} was detected by western blot. Captured GST fusion proteins were detected with Ponceau S.

(B) Top: schematic of mSIRT1. In the bottom panel, His_6-PACS-2_{FBR} was incubated with GST or GST-SIRT1 constructs, and interacting His_6-PACS-2_{FBR} was detected by western blot as in (A).

(C) GST-Ac-p53 (see Experimental Procedures) was incubated with 0.5 mM NAD^+ and His_6-tagged SIRT1 or SIRT1-ΔNT together with increasing amounts of His_6-PACS-2_{FBR} as indicated. The amount of Ac-p53 (K_{382}) was quantified and presented as percent acetylation. Error bars represent mean ± SEM from four independent experiments.

(D) GST-Ac-p53 was incubated with 0.5 mM NAD^+ and His_6-SIRT1 together with increasing amounts of His_6-PACS-1 or PACS-2 as indicated. The amount of Ac-p53 (K_{382}) was quantified as in (C).

See also Figure S4.

tumor-suppressive functions (Herranz and Serrano, 2010; Roth and Chen, 2014). These opposing roles for SIRT1 are likely manifest through extensive SIRT1 substrates together with the ability of SIRT1 to differentially affect the cellular response to chemotherapeutics. For example, in cells exposed to high concentrations of chemotherapeutics, overexpressed SIRT1 represses induction of p53 target genes and reduces apoptosis (Luo et al., 2001; Vaziri et al., 2001). By contrast, and similar to our findings reported here, viability of HCT116 cells and other cell lines exposed to therapeutic doses of Dox is reduced by SIRT1 overexpression or treatment with SIRT1 activators but is increased by addition of EX-527 (Shin et al., 2014). Together, these findings suggest that the roles of SIRT1 in the cellular response to DNA damage are complex and manifest in a dose- and context-dependent manner.

In contrast to other sirtuin family members, SIRT1 additionally possesses N- and C-terminal extensions containing autoregulatory domains and binding sites for SIRT1 modulators (Hasegawa

and Yoshikawa, 2008; Kang et al., 2011; Kim et al., 2007, 2008; Liu et al., 2011; Zhao et al., 2008). The SIRT1 C-terminal extension contributes to the K_M for NAD^+ and contains an autoregulatory segment that binds the core domain, which is required for catalytic activity (Kang et al., 2011; Pan et al., 2012). The SIRT1 N-terminal extension contributes to k_{cat} and regulates allosteric binding of sirtuin-activating compounds (Hubbard et al., 2013). Like PACS-2, the SIRT1 activator AROS binds the SIRT1 NT but has an opposing role on p53 regulation. Whereas PACS-2 inhibits SIRT1 to increase p53 acetylation, p21 induction, and p21-dependent cell-cycle arrest, AROS activates SIRT1 to decrease p53 deacetylation and consequently blunt p21 induction and cell-cycle arrest (Kim et al., 2007). By contrast, DBC1 binds to the SIRT1 catalytic (sirtuin) domain, and, unlike PACS-2, small interfering RNA (siRNA) knockdown of this inhibitor blunts the induction of several proapoptotic p53 targets, including PUMA, Bax, and Bim, and paradoxically increases in the cell-cycle inhibitor GADD45a (Kim et al., 2008; Yuan et al., 2012; Zhao et al., 2008). Correspondingly, DBC1 knockdown reduces apoptosis, albeit with high concentrations of chemotherapeutics. However, the extent to which the cytoprotective effects of DBC1 knockdown following DNA damage result from increased SIRT1 versus the selective reduction of proapoptotic genes warrants further investigation. Moreover, the blunted acetylation of p53 in Pacs-$2^{-/-}$ thymocytes following DNA damage despite similar expression of DBC1 (Figure 2A) suggests that PACS-2 and DBC1 regulate SIRT1 independently and have dynamic and concerted roles in resolving the DNA damage response.

Acetylation-dependent transactivation of p53 involves a C-terminal cluster of six lysine residues and three additional sites within the core domain (Brooks and Gu, 2011). p300 acetylates the p53 C-terminal cluster, including Lys_{382}, preventing MDM2-mediated ubiquitylation and promoting p53 transactivation (Lee et al., 2010; Luo et al., 2004; Tang et al., 2008; Wang et al., 2008). However, the PACS-2-mediated acetylation of p53 Lys_{382} alone cannot explain the requirement for PACS-2 in the expression of a subset of p53 target genes. Interestingly, the DNA damage-mediated induction of p21 but not Bax additionally requires recruitment of BRCA1 and CARM1, which methylates p300 to stabilize the transcriptional complex (Lee et al., 2011). In contrast to p21, the p53-dependent induction of proapoptotic PUMA requires Tip60 or MOF-mediated acetylation of Lys_{120} (Sykes et al., 2006; Tang et al., 2006). Because SIRT1 also regulates these two acetyltransferases, it will be important to determine whether PACS-2 regulates the action of SIRT1 against one or both enzymes or whether PACS-2 mediates recruitment of BRCA1/CARM1 to induce p21 (Peng et al., 2012).

Cytoplasmic PACS-2 mediates MAM formation, autophagy, and protein traffic in the secretory and endocytic pathways (Atkins et al., 2008; Betz et al., 2013; Dikeakos et al., 2012; Hamasaki et al., 2013; Köttgen et al., 2005; Simmen et al., 2005). In response to TRAIL, PACS-2 switches to a proapoptotic effector independent of p53 status that coordinates trafficking steps leading to Bim- and Bid-dependent lysosomal and mitochondria membrane permeabilization, respectively, to trigger activation of executioner caspases (Aslan et al., 2009; Werneburg et al., 2012). It was therefore surprising that PACS-2 has seemingly opposing roles in TRAIL-induced versus DNA damage-induced apoptosis where in response to DNA damage, nuclear PACS-2 promotes p53 transactivation to induce p21-dependent cell-cycle arrest (Figures 4, 5, and 6). Recent studies, however, suggest that TRAIL selectively kills arrested cells (Ehrhardt et al., 2013). Thus, PACS-2-mediated cell-cycle arrest may enhance PACS-2-dependent TRAIL-induced apoptosis. Therefore, it will be important to determine the stoichiometry of nuclear PACS-2 and SIRT1 that promotes p21 induction as well as the extent to which SIRT1 interaction involves preexisting nuclear PACS-2 versus PACS-2 translocated from the cytoplasm in response to DNA damage.

Our data identify PACS-2 as a member of an emerging collection of proteins with established roles in regulating both secretory pathway traffic and nuclear gene expression (Copley, 2012). Phylogenetic studies indicate that the PACS genes appeared first in metazoans (Youker et al., 2009). Although lower metazoans express a single PACS gene, separate PACS-1 and PACS-2 genes are predicted to have arisen in higher metazoans by gene duplication. Sequence alignment suggests that PACS-1 and PACS-2 underwent evolutionary adaptation with the acquisition of nuclear-trafficking motifs (see Figure 3C). Consistent with this model, *C. elegans* PACS failed to accumulate in the nucleus in LMB-treated cells (Figure 3C). This evolutionary acquisition of nuclear-trafficking functions parallels the role of p53 in directing cell-cycle arrest. p53 was found to promote apoptosis in worms and flies but in higher metazoans was found to additionally induce p21-dependent cell-cycle arrest (Lu et al., 2009). These findings raise the possibility that the ability of PACS-2 to traffic to the nucleus resulted from evolutionary adaptation required to support the more complex demands of p53 to resolve the DNA damage response.

In summary, our data demonstrate that the multifunctional protein PACS-2 shuttles to the nucleus and directly inhibits SIRT1-mediated deacetylation of p53, thereby controlling the SIRT1-p53-p21 axis to modulate the DNA damage response. Our findings, together with the broad and important role of SIRT1 in controlling pathways associated with cancer, aging, and metabolism, suggest that a more complete understanding of the regulation of SIRT1 is warranted to better understand the complex role of this deacetylase in controlling homeostasis and disease.

EXPERIMENTAL PROCEDURES

Experimental Animals

The Oregon Health & Science University (OHSU) Department of Comparative Medicine and the University of Pittsburgh Division of Laboratory Animal Resources approved all animal studies. Pacs-$2^{-/-}$ mice (Aslan et al., 2009) were maintained on a C57BL/6 background with more than ten backcrosses. Mice were irradiated using a J.L. Shepherd & Associates Mark I Model 30 cesium irradiator (1.475 Gy/min) in a Plexiglas pie plate rotating at 7 rpm. Where indicated, WT and Pacs-$2^{-/-}$ mice were injected with 50 mg/kg BrdU and immediately exposed to 15 Gy whole-body irradiation (WBI). At 48 hr following labeling, a 3 cm segment of ileum just proximal to the cecum was processed for immunohistochemistry (IHC) by the OHSU Histopathology Core.

Antibodies, Chemicals, Plasmids, and siRNAs

See Supplemental Experimental Procedures.

Cell Harvest and Tissue Processing

HCT116 cell lines (provided with permission from B. Vogelstein) and U2OS and 293T cells were cultured in Dulbecco's modified Eagle's medium plus 10% fetal bovine serum (FBS). For most experiments, cells were harvested in modified radioimmunoprecipitation assay buffer (mRIPA) (50 mM Tris-HCl [pH 8.0] plus 1% NP-40, 1% deoxycholate, and 150 mM NaCl) containing proteinase inhibitors (0.5 mM phenylmethanesulfonylfluoride, 0.1 μM each of aprotinin, E-64, and leupeptin) and phosphatase inhibitors (1 mM Na_3VO_4 and 20 mM NaF). For monitoring Ac-p53, cells were harvested in Ac lysis buffer (20 mM Tris-HCl [pH 7.6] plus 0.5% NP-40, 150 mM NaCl, 1 mM EDTA, 1 mM dithiothreitol [DTT], and 5 μM TSA) containing protease inhibitors and phosphatase inhibitors. Mouse tissues were homogenized in RIPA (50 mM Tris-HCl [pH 8.0] plus 150 mM NaCl, 1% NP-40, 1% deoxycholate, and 0.1% SDS) containing protease/phosphatase inhibitors using a motorized Teflon glass homogenizer. Protein concentration was determined according to manufacturer's instructions (#500-0006; Bio-Rad).

Flow Cytometry Analyses

Flow cytometry was performed on FACSCalibur or Accuri C6 (BD Biosciences) flow cytometers. Data were analyzed using FCS Express (v.3.0; BD Biosciences).

Cell-Cycle Analysis

HCT116 cells were nucleofected (Amaxa) on days 0 and 2 with the indicated siRNAs. On day 4, the nucleofected cells were synchronized by serum deprivation (0.1% FBS) for 24 hr and stimulated to reenter the cell cycle by addition of 10% FBS in the presence of 10 μM BrdU and treated or not with 0.5 μM Dox or 10 μM EX-527 for an additional 24 hr as indicated. EX-527 was used in these experiments because it could selectively inhibit SIRT1 following serum deprivation, thereby avoiding nutrient-affected changes in SIRT1 prior to DNA damage (Nemoto et al., 2004). Cells were processed according to the manufacturer's instructions (#559619; BD Pharmingen), and flow cytometry was performed as above.

qPCR Analysis

Cell culture studies were performed using subconfluent HCT116 cells, transfected with siRNAs, synchronized with 1% serum, and refed with 10% serum in the absence or presence of Dox as indicated. RNA was isolated according to manufacturer's instructions using TRIzol (#15596-026; Sigma-Aldrich) for mouse tissues and RNeasy (#74104; QIAGEN) for cell culture. RNA was reverse transcribed using the SuperScript III First-Strand cDNA Synthesis Kit (#18080-051; Invitrogen). Reactions were performed in a StepOne Real-Time PCR System with the Power SYBR Green PCR Master Mix (#4368706; Applied Biosystems) using the primer pairs listed in Supplemental Experimental Procedures. All reactions were performed in triplicate.

ChIP Analysis

ChIP experiments were performed according to Mahata et al. (2012) with modifications as detailed in Supplemental Experimental Procedures.

Baculovirus

Full-length human PACS-1 (hPACS-1)- and hPACS-2-coding sequences containing a C-terminal His tag were subcloned into pVL1392 (BD Biosciences) to create high-titer recombinant baculoviruses (BV:His_6-PACS-1 and BV:His_6-PACS-2) in Sf9 insect cells according to the manufacturer's protocol (BD Biosciences). Sf9 cells were cultured for 72 hr with BV:His_6-PACS-2 or BV:His_6-PACS-1 and dounce homogenized in harvest buffer (50 mM $NaHPO_4$ [pH 7.4] and 300 mM NaCl). Lysates were clarified by centrifugation (20,000 rpm, 20 min). His_6-tagged proteins were purified using Ni^{2+}-NTA agarose (QIAGEN) and dialyzed against PBS.

In Vitro Binding

Glutathione S-transferase (GST) proteins were preincubated with Glutathione Sepharose 4B (GE Healthcare) in binding buffer (20 mM Tris-HCl [pH 7.9], 150 mM NaCl, 0.1% NP-40, 0.1 mM EDTA, and 0.3 mM DTT), mixed with His_6-constructs (30 min, room temperature), washed 3× (20 mM Tris-HCl [pH 7.9], 300 mM NaCl, 0.1% NP-40, 0.1 mM EDTA, and 3 mM DTT), and analyzed by western blot using anti-His_6. For SIRT1 and full-length PACS interactions, His_6-PACS-1 or His_6-PACS-2 expressed in baculovirus-infected Sf9 cells was mixed with GST or GST-$SIRT1_{1–737}$ preincubated with Glutathione Sepharose 4B and processed as above.

In Vitro Deacetylase Assays

Substrate preparation and in vitro deacetylation assays were performed as described (Aslan et al., 2009; Kang et al., 2009; Simmen et al., 2005). Briefly, purified GST-$hp53_{373–385}$ was acetylated by His_6-$PCAF_{352–832}$ in HAT buffer (50 mM Tris-HCl [pH 8.0], 10% glycerol, 0.1 mM EDTA, and 1.0 M DTT) with 5 mM acetyl coenzyme A (Millipore). For assays with full-length PACS proteins, purified His_6-mSIRT1 was preincubated with GST-Ac-p53 and full-length His_6-PACS-1 or PACS-2 in deacetylase buffer (50 mM Tris-HCl [pH 8.0] plus 150 mM NaCl, 10 mM $MgCl_2$, 1 mM DTT, and protease inhibitors) for 30 min. Assays using $PACS\text{-}2_{FBR}$ were conducted in binding buffer (see above). Reactions were initiated with 0.5 mM NAD^+ (Millipore) and run for 1 hr to overnight at 37°C.

Microscopy

U2OS cells were transfected (FuGENE 6) with the indicated plasmids, and images were acquired on a high-resolution, wide-field Core DeltaVision System (Applied Precision) as described (Dikeakos et al., 2012). Nuclear and cytoplasmic fluorescent signal was determined using softWoRx Explorer 2.0 (Applied Precision) also as described (Dikeakos et al., 2012). Briefly, for each cell counted, the mCherry or DAPI fluorescent signal was quantified from a precise region of interest over the nucleus, cytoplasm, and extracellular space. The fluorescent signal in each channel was automatically captured, and the signal from the extracellular space was subtracted from the nuclear and cytoplasmic signals. The nuclear signal was then divided by the total (nuclear plus cytoplasmic) signal. Statistical significance was determined using a two-sided unpaired Student's t test with unequal variance.

Nuclear Fractionation

Cells were harvested in Buffer 1 (50 mM Tris-HCl [pH 7.9] plus 10 mM KCl, 1 mM EDTA, 0.2% NP-40, 10% glycerol, and protease inhibitors) and centrifuged (3.3k × *g*, 3 min, 4°C). The nuclear pellet was lysed with Buffer 2 (20 mM HEPES [pH 7.9] plus 400 mM NaCl, 10 mM KCl, 1% NP-40, 20% glycerol, 1 mM EDTA, and protease inhibitors) for 20 min at 4°C, then centrifuged (16.1k × *g*, 10 min, 4°C). Soluble nuclear and cytoplasmic fractions were immunoprecipitated with anti-FLAG-agarose or anti-SIRT1 (H-300) antibodies, and immune complexes were captured with Protein G Sepharose (Invitrogen) for 2 hr at 4°C, washed 3× in wash buffer (20 mM Tris-HCl [pH 7.6] plus 0.5% NP-40, 150 mM NaCl, and 1 mM EDTA), and eluted in SDS sample buffer prior to western blot.

SUPPLEMENTAL INFORMATION

Supplemental Information includes Supplemental Experimental Procedures, four figures, and two tables and can be found with this article online at http://dx.doi.org/10.1016/j.celrep.2014.07.049.

AUTHOR CONTRIBUTIONS

K.M.A., L.L.T., J.B.-G., L.T., S.A., J.Y., and J.D.D. conceived and designed the experiments. K.M.A., L.L.T., J.B.-G., L.T., S.A., and J.Y. performed the experiments. K.M.A., L.L.T., J.B.-G., L.T., S.A., J.Y., H.K., J.H.C., and J.D.D. analyzed the data. G.T. wrote the paper. K.M.A., L.L.T., and J.B.-G. edited the paper. L.T. assembled the artwork. All the authors approved the final version of the manuscript.

ACKNOWLEDGMENTS

The authors thank B. Vogelstein, L. Zhang, J. Yu, D. Sieburth, G.V. Thomas, P. Stork, and J. Denu for reagents and J. Yu, M. Dai, V. Procaccia, T. Smithgall, J. A. Tanyi, and J. Moroco for advice and assistance with experiments. This work

was supported by NIH R01 CA151564 and awards from the Knight Cancer Institute and the University of Pittsburgh (to G.T). K.M.A. is a Rubinstein Radiation Research Scholar and was supported by RSNA RMS1112 and the N.L. Tartar Foundation.

Received: June 26, 2013
Revised: July 3, 2014
Accepted: July 25, 2014
Published: August 21, 2014

REFERENCES

Abbas, T., and Dutta, A. (2009). p21 in cancer: intricate networks and multiple activities. Nat. Rev. Cancer *9*, 400–414.

Aslan, J.E., You, H., Williamson, D.M., Endig, J., Youker, R.T., Thomas, L., Shu, H., Du, Y., Milewski, R.L., Brush, M.H., et al. (2009). Akt and 14-3-3 control a PACS-2 homeostatic switch that integrates membrane traffic with TRAIL-induced apoptosis. Mol. Cell *34*, 497–509.

Atkins, K.M., Thomas, L., Youker, R.T., Harriff, M.J., Pissani, F., You, H., and Thomas, G. (2008). HIV-1 Nef binds PACS-2 to assemble a multikinase cascade that triggers major histocompatibility complex class I (MHC-I) down-regulation: analysis using short interfering RNA and knock-out mice. J. Biol. Chem. *283*, 11772–11784.

Baptiste-Okoh, N., Barsotti, A.M., and Prives, C. (2008). Caspase 2 is both required for p53-mediated apoptosis and downregulated by p53 in a p21-dependent manner. Cell Cycle *7*, 1133–1138.

Betz, C., Stracka, D., Prescianotto-Baschong, C., Frieden, M., Demaurex, N., and Hall, M.N. (2013). Feature Article: mTOR complex 2-Akt signaling at mitochondria-associated endoplasmic reticulum membranes (MAM) regulates mitochondrial physiology. Proc. Natl. Acad. Sci. USA *110*, 12526–12534.

Brooks, C.L., and Gu, W. (2009). How does SIRT1 affect metabolism, senescence and cancer? Nat. Rev. Cancer *9*, 123–128.

Brooks, C.L., and Gu, W. (2011). The impact of acetylation and deacetylation on the p53 pathway. Protein Cell *2*, 456–462.

Cheng, H.L., Mostoslavsky, R., Saito, S., Manis, J.P., Gu, Y., Patel, P., Bronson, R., Appella, E., Alt, F.W., and Chua, K.F. (2003). Developmental defects and p53 hyperacetylation in Sir2 homolog (SIRT1)-deficient mice. Proc. Natl. Acad. Sci. USA *100*, 10794–10799.

Cohen, H.Y., Miller, C., Bitterman, K.J., Wall, N.R., Hekking, B., Kessler, B., Howitz, K.T., Gorospe, M., de Cabo, R., and Sinclair, D.A. (2004). Calorie restriction promotes mammalian cell survival by inducing the SIRT1 deacetylase. Science *305*, 390–392.

Copley, S.D. (2012). Moonlighting is mainstream: paradigm adjustment required. BioEssays *34*, 578–588.

Dikeakos, J.D., Thomas, L., Kwon, G., Elferich, J., Shinde, U., and Thomas, G. (2012). An interdomain binding site on HIV-1 Nef interacts with PACS-1 and PACS-2 on endosomes to down-regulate MHC-I. Mol. Biol. Cell *23*, 2184–2197.

Ehrhardt, H., Wachter, F., Grunert, M., and Jeremias, I. (2013). Cell cycle-arrested tumor cells exhibit increased sensitivity towards TRAIL-induced apoptosis. Cell Death Dis. *4*, e661.

Gu, W., and Roeder, R.G. (1997). Activation of p53 sequence-specific DNA binding by acetylation of the p53 C-terminal domain. Cell *90*, 595–606.

Hamasaki, M., Furuta, N., Matsuda, A., Nezu, A., Yamamoto, A., Fujita, N., Oomori, H., Noda, T., Haraguchi, T., Hiraoka, Y., et al. (2013). Autophagosomes form at ER-mitochondria contact sites. Nature *495*, 389–393.

Hasegawa, K., and Yoshikawa, K. (2008). Necdin regulates p53 acetylation via Sirtuin1 to modulate DNA damage response in cortical neurons. J. Neurosci. *28*, 8772–8784.

Haupt, S., Louria-Hayon, I., and Haupt, Y. (2003). P53 licensed to kill? Operating the assassin. J. Cell. Biochem. *88*, 76–82.

Herranz, D., and Serrano, M. (2010). SIRT1: recent lessons from mouse models. Nat. Rev. Cancer *10*, 819–823.

Hill, R., Madureira, P.A., Waisman, D.M., and Lee, P.W. (2011). DNA-PKCS binding to p53 on the p21WAF1/CIP1 promoter blocks transcription resulting in cell death. Oncotarget *2*, 1094–1108.

Hubbard, B.P., Gomes, A.P., Dai, H., Li, J., Case, A.W., Considine, T., Riera, T.V., Lee, J.E., E, S.Y., Lamming, D.W., et al. (2013). Evidence for a common mechanism of SIRT1 regulation by allosteric activators. Science *339*, 1216–1219.

Ifeadi, V., and Garnett-Benson, C. (2012). Sub-lethal irradiation of human colorectal tumor cells imparts enhanced and sustained susceptibility to multiple death receptor signaling pathways. PLoS One *7*, e31762.

Ju, Z., Choudhury, A.R., and Rudolph, K.L. (2007). A dual role of p21 in stem cell aging. Ann. N Y Acad. Sci. *1100*, 333–344.

Kang, H., Jung, J.W., Kim, M.K., and Chung, J.H. (2009). CK2 is the regulator of SIRT1 substrate-binding affinity, deacetylase activity and cellular response to DNA-damage. PLoS One *4*, e6611.

Kang, H., Suh, J.Y., Jung, Y.S., Jung, J.W., Kim, M.K., and Chung, J.H. (2011). Peptide switch is essential for Sirt1 deacetylase activity. Mol. Cell *44*, 203–213.

Kim, E.J., Kho, J.H., Kang, M.R., and Um, S.J. (2007). Active regulator of SIRT1 cooperates with SIRT1 and facilitates suppression of p53 activity. Mol. Cell *28*, 277–290.

Kim, J.E., Chen, J., and Lou, Z. (2008). DBC1 is a negative regulator of SIRT1. Nature *451*, 583–586.

Komarova, E.A., Kondratov, R.V., Wang, K., Christov, K., Golovkina, T.V., Goldblum, J.R., and Gudkov, A.V. (2004). Dual effect of p53 on radiation sensitivity in vivo: p53 promotes hematopoietic injury, but protects from gastro-intestinal syndrome in mice. Oncogene *23*, 3265–3271.

Köttgen, M., Benzing, T., Simmen, T., Tauber, R., Buchholz, B., Feliciangeli, S., Huber, T.B., Schermer, B., Kramer-Zucker, A., Höpker, K., et al. (2005). Trafficking of TRPP2 by PACS proteins represents a novel mechanism of ion channel regulation. EMBO J. *24*, 705–716.

Kruse, J.P., and Gu, W. (2009). Modes of p53 regulation. Cell *137*, 609–622.

Kumamoto, K., Spillare, E.A., Fujita, K., Horikawa, I., Yamashita, T., Appella, E., Nagashima, M., Takenoshita, S., Yokota, J., and Harris, C.C. (2008). Nutlin-3a activates p53 to both down-regulate inhibitor of growth 2 and up-regulate mir-34a, mir-34b, and mir-34c expression, and induce senescence. Cancer Res. *68*, 3193–3203.

Kwon, H.S., and Ott, M. (2008). The ups and downs of SIRT1. Trends Biochem. Sci. *33*, 517–525.

la Cour, T., Kiemer, L., Mølgaard, A., Gupta, R., Skriver, K., and Brunak, S. (2004). Analysis and prediction of leucine-rich nuclear export signals. Protein Eng. Des. Sel. *17*, 527–536.

Lee, C.W., Ferreon, J.C., Ferreon, A.C., Arai, M., and Wright, P.E. (2010). Graded enhancement of p53 binding to CREB-binding protein (CBP) by multisite phosphorylation. Proc. Natl. Acad. Sci. USA *107*, 19290–19295.

Lee, Y.H., Bedford, M.T., and Stallcup, M.R. (2011). Regulated recruitment of tumor suppressor BRCA1 to the p21 gene by coactivator methylation. Genes Dev. *25*, 176–188.

Leibowitz, B.J., Qiu, W., Liu, H., Cheng, T., Zhang, L., and Yu, J. (2011). Uncoupling p53 functions in radiation-induced intestinal damage via PUMA and p21. Mol. Cancer Res. *9*, 616–625.

Li, J., Hassan, G.S., Williams, T.M., Minetti, C., Pestell, R.G., Tanowitz, H.B., Frank, P.G., Sotgia, F., and Lisanti, M.P. (2005). Loss of caveolin-1 causes the hyper-proliferation of intestinal crypt stem cells, with increased sensitivity to whole body gamma-radiation. Cell Cycle *4*, 1817–1825.

Liu, X., Wang, D., Zhao, Y., Tu, B., Zheng, Z., Wang, L., Wang, H., Gu, W., Roeder, R.G., and Zhu, W.G. (2011). Methyltransferase Set7/9 regulates p53 activity by interacting with Sirtuin 1 (SIRT1). Proc. Natl. Acad. Sci. USA *108*, 1925–1930.

Lu, W.J., Amatruda, J.F., and Abrams, J.M. (2009). p53 ancestry: gazing through an evolutionary lens. Nat. Rev. Cancer *9*, 758–762.

Luo, J., Nikolaev, A.Y., Imai, S., Chen, D., Su, F., Shiloh, A., Guarente, L., and Gu, W. (2001). Negative control of p53 by Sir2alpha promotes cell survival under stress. Cell *107*, 137–148.

Luo, J., Li, M., Tang, Y., Laszkowska, M., Roeder, R.G., and Gu, W. (2004). Acetylation of p53 augments its site-specific DNA binding both in vitro and in vivo. Proc. Natl. Acad. Sci. USA *101*, 2259–2264.

Mahata, B., Sundqvist, A., and Xirodimas, D.P. (2012). Recruitment of RPL11 at promoter sites of p53-regulated genes upon nucleolar stress through NEDD8 and in an Mdm2-dependent manner. Oncogene *31*, 3060–3071.

Mantel, C., and Broxmeyer, H.E. (2008). Sirtuin 1, stem cells, aging, and stem cell aging. Curr. Opin. Hematol. *15*, 326–331.

Mirzayans, R., Andrais, B., Scott, A., and Murray, D. (2012). New insights into p53 signaling and cancer cell response to DNA damage: implications for cancer therapy. J. Biomed. Biotechnol. *2012*, 170325.

Napper, A.D., Hixon, J., McDonagh, T., Keavey, K., Pons, J.F., Barker, J., Yau, W.T., Amouzegh, P., Flegg, A., Hamelin, E., et al. (2005). Discovery of indoles as potent and selective inhibitors of the deacetylase SIRT1. J. Med. Chem. *48*, 8045–8054.

Nemoto, S., Fergusson, M.M., and Finkel, T. (2004). Nutrient availability regulates SIRT1 through a forkhead-dependent pathway. Science *306*, 2105–2108.

Pan, M., Yuan, H., Brent, M., Ding, E.C., and Marmorstein, R. (2012). SIRT1 contains N- and C-terminal regions that potentiate deacetylase activity. J. Biol. Chem. *287*, 2468–2476.

Peng, L., Ling, H., Yuan, Z., Fang, B., Bloom, G., Fukasawa, K., Koomen, J., Chen, J., Lane, W.S., and Seto, E. (2012). SIRT1 negatively regulates the activities, functions, and protein levels of hMOF and TIP60. Mol. Cell. Biol. *32*, 2823–2836.

Roth, M., and Chen, W.Y. (2014). Sorting out functions of sirtuins in cancer. Oncogene *33*, 1609–1620.

Seoane, J., Le, H.V., and Massagué, J. (2002). Myc suppression of the p21(Cip1) Cdk inhibitor influences the outcome of the p53 response to DNA damage. Nature *419*, 729–734.

Shin, D.H., Choi, Y.J., and Park, J.W. (2014). SIRT1 and AMPK mediate hypoxia-induced resistance of non-small cell lung cancers to cisplatin and doxorubicin. Cancer Res. *74*, 298–308.

Simmen, T., Aslan, J.E., Blagoveshchenskaya, A.D., Thomas, L., Wan, L., Xiang, Y., Feliciangeli, S.F., Hung, C.H., Crump, C.M., and Thomas, G. (2005). PACS-2 controls endoplasmic reticulum-mitochondria communication and Bid-mediated apoptosis. EMBO J. *24*, 717–729.

Solomon, J.M., Pasupuleti, R., Xu, L., McDonagh, T., Curtis, R., DiStefano, P.S., and Huber, L.J. (2006). Inhibition of SIRT1 catalytic activity increases p53 acetylation but does not alter cell survival following DNA damage. Mol. Cell. Biol. *26*, 28–38.

Sperka, T., Wang, J., and Rudolph, K.L. (2012). DNA damage checkpoints in stem cells, ageing and cancer. Nat. Rev. Mol. Cell Biol. *13*, 579–590.

Sullivan, J.M., Jeffords, L.B., Lee, C.L., Rodrigues, R., Ma, Y., and Kirsch, D.G. (2012). p21 protects "Super p53" mice from the radiation-induced gastrointestinal syndrome. Radiat. Res. *177*, 307–310.

Suzuki, A., Kawano, H., Hayashida, M., Hayasaki, Y., Tsutomi, Y., and Akahane, K. (2000). Procaspase 3/p21 complex formation to resist fas-mediated cell death is initiated as a result of the phosphorylation of p21 by protein kinase A. Cell Death Differ. *7*, 721–728.

Sykes, S.M., Mellert, H.S., Holbert, M.A., Li, K., Marmorstein, R., Lane, W.S., and McMahon, S.B. (2006). Acetylation of the p53 DNA-binding domain regulates apoptosis induction. Mol. Cell *24*, 841–851.

Tang, Y., Luo, J., Zhang, W., and Gu, W. (2006). Tip60-dependent acetylation of p53 modulates the decision between cell-cycle arrest and apoptosis. Mol. Cell *24*, 827–839.

Tang, Y., Zhao, W., Chen, Y., Zhao, Y., and Gu, W. (2008). Acetylation is indispensable for p53 activation. Cell *133*, 612–626.

Vaziri, H., Dessain, S.K., Ng Eaton, E., Imai, S.I., Frye, R.A., Pandita, T.K., Guarente, L., and Weinberg, R.A. (2001). hSIR2(SIRT1) functions as an NAD-dependent p53 deacetylase. Cell *107*, 149–159.

Wang, H., Zhao, Y., Li, L., McNutt, M.A., Wu, L., Lu, S., Yu, Y., Zhou, W., Feng, J., Chai, G., et al. (2008). An ATM- and Rad3-related (ATR) signaling pathway and a phosphorylation-acetylation cascade are involved in activation of p53/p21Waf1/Cip1 in response to 5-aza-2′-deoxycytidine treatment. J. Biol. Chem. *283*, 2564–2574.

Werneburg, N.W., Bronk, S.F., Guicciardi, M.E., Thomas, L., Dikeakos, J.D., Thomas, G., and Gores, G.J. (2012). Tumor necrosis factor-related apoptosis-inducing ligand (TRAIL) protein-induced lysosomal translocation of proapoptotic effectors is mediated by phosphofurin acidic cluster sorting protein-2 (PACS-2). J. Biol. Chem. *287*, 24427–24437.

Youker, R.T., Shinde, U., Day, R., and Thomas, G. (2009). At the crossroads of homoeostasis and disease: roles of the PACS proteins in membrane traffic and apoptosis. Biochem. J. *421*, 1–15.

Yu, J., Wang, Z., Kinzler, K.W., Vogelstein, B., and Zhang, L. (2003). PUMA mediates the apoptotic response to p53 in colorectal cancer cells. Proc. Natl. Acad. Sci. USA *100*, 1931–1936.

Yuan, J., Luo, K., Liu, T., and Lou, Z. (2012). Regulation of SIRT1 activity by genotoxic stress. Genes Dev. *26*, 791–796.

Zhao, W., Kruse, J.P., Tang, Y., Jung, S.Y., Qin, J., and Gu, W. (2008). Negative regulation of the deacetylase SIRT1 by DBC1. Nature *451*, 587–590.

Zilfou, J.T., and Lowe, S.W. (2009). Tumor suppressive functions of p53. Cold Spring Harb. Perspect. Biol. *1*, a001883.